Mechanics of Advanced Composite Structures 8 (2021) 33-40

Semnan University

Mechanics of Advanced Composite Structures

journal homepage: http://MACS.journals.semnan.ac.ir

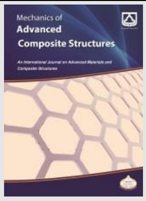

On the Nonlinear Dynamics of an Energy Harvesting Device Based on Magnetostriction

P. Abdollahzadeh, S. Azizi, S. H. Hoseini*

Faculty of Mechanical Engineering, Urmia University of Technology, Urmia, West Azarbayjan, Iran

KEYWORDS

Energy harvesting
Magnetostrictive material
Base excitation
Galerkin method
Nonlinear Dynamics

ABSTRACT

In this paper, a magnetostrictive material (MSM)-based energy harvesting device is proposed. The device is made up of a steel beam laminated with Metglas 2605sc as the magnetostrictive material; the device undergoes mechanical strain due to the external base excitation. The mechanical strain yields in a magnetic field around the beam. A pickup coil is surrounded around the beam which converts the magnetic field into electrical current. The equation of motion is derived based on the nonlinear Euler-Bernoulli beam theory to account for large deflections. Kirchhoff and Faraday's laws are also benefited to couple the mechanical, magnetic and electrical fields. The equation is discretized based on the Galerkin method and numerically integrated over time. Energy conservation is examined and the response in the frequency domain is obtained. In the case of initial displacement, in the absence of mechanical damping, vibration amplitude attenuates as the electrical current induces in the pickup coil; this was attributed to the attenuation of the total mechanical energy of the beam as it was harvested from the pickup coil. The temporal response was fitted to that of a single degree of freedom mass-spring-damped and the equivalent damping ratio was determined. The attenuation rate was studied with different values of resistance and the number of turns in the pickup coil and the relation between these two factors was obtained to maximize the output electrical power.

1. Introduction

Magnetostriction first reported by J. Joule [1] in 1842 refers to a property of ferromagnetic materials that causes them to change their shape or dimension during magnetization. These shape changes are due to the rotation and reorientation of small magnetic domains in material. Villary Effect is a phenomenon based on the change of magnetic flux in the sample that creates a magnetic field around it once subjected to mechanical stress [2]; these materials are then used in many sensing and actuating applications, because of their excellent features. A.G. Olabi [3] had reviewed several applications of these materials.

Due to increasing demand for energy and development of long-lasting devices working in fields where neither energy supplies exist, nor can batteries be recharged, energy harvesting is a recently focused research field. It can be used in many practical fields such as wireless sensor networks (WSN), health monitoring, self-powered sensors, and wearable electronics [4]. Energy harvesting alludes to the process in which electrical energy is derived from external ambient sources such as solar, thermal, mechanical, and so on. In the context of mechanical energy harvesters itself, several types have been investigated while the electrostatic, electromagnetic and piezoelectric are the most common mechanisms. Among these, piezoelectric harvesters are the most widely studied ones, although they have some inherent shortcomings including its brittleness, aging, and depolarization [4]. Garg et al. [5] studied the nonlinear dynamics of parametrically-exited piezoelectric harvesters. Rojas et al. [6] accounted for the size dependency of harvesters and considered atomic interaction of them and proposed a modified continuum model. Leadenham et al. [7] not only did derive a lumped-parameter model of the nonlinear resonant behavior of the harvester but also studied the AC-DC convertor with non-ideal diodes. Further, Faroughi et al. [8] modeled non-

* Corresponding author. Tel.: +98-44-33728181 ; Fax: +98-44-33728183
E-mail address: s.hamedhoseini@uut.ac.ir

DOI: 10.22075/MACS.2020.19529.1233
Received 2020-01-11; Received in revised form 2020-04-28; Accepted 2020-06-19

uniform flexoelectric cantilever energy harvester using classic continuum theories and learned that the geometric non-uniformity of the harvester beams increases the harvested power.

Another application of MSM materials is in energy harvesting devices in which the magnetostriction property of these materials is used to convert mechanical energy to the magnetic field according to Villay effect. Higher power density at lower frequencies than other types of harvesters is one of MSM harvester's preferences, which is a challenging dilemma since most parts of ambient vibrations are of this range [9,10,11]. Yet most of the studies in this context were about proving the possibility of scavenging energy based on MSM harvesters, experimentally rather than analyzing them analytically. M. Staley et al. [12] tested two samples of Terfenol-D and Iron-Gallium, excited by a mechanical shaker and studied the electrical output dependency on mechanical input under different conditions. S. Mohammadi et al. [10] performed a parametrical study to optimize power in an energy harvester beam equipped with metglas. A. Adly et al. [13] performed experimental tests on their proposed model and suggested a potentially more complex model be defined to convey more accurate analysis because of the nonlinear behavior they observed in their experiments. D. Davino et al. [14] discussed the constitutive modeling of magnetostrictive energy harvesters and mainly the hysteresis losses and analyzed power optimization in them [15]. H. Talleb et al. [16] presented a Finite Element Method to capture characterizations of a magnetostrictive-piezoelectric harvester. N. Neirla et al. [17] also offered an iterative FE scheme to study lately mentioned magnetostrictive-piezoelectric harvester which also allows changing geometry. M. Borowiec et al. [18] analyzed different shapes of energy harvesting beams for different resonant frequencies. H. Jafari et al. [19] theoretically investigated the dynamics of steel beam laminated by metglas employing linear Euler-Bernoulli beam theory and concluded Lorenzian response of non-dimensional damping coefficient in terms of load resistance and also the preference of MSM harvester to piezoelectric one for low-frequency base excitation applications. The more is the motion amplitude; the more is the harvested energy. In this study, large deformation motion of a cantilever steel beam laminated by Metglas and wounded by a pickup coil is investigated. The device undergoes mechanical strain due to external base excitation. The mechanical strain in the Metglas yields in a magnetic field around the cantilever beam, and accordingly an electrical current is induced in the coil. Since the beam is slim and undergoes large deflections, the nonlinear Euler-Bernoulli beam theory is chosen for analysis of the dynamical behavior of the energy harvester and the appropriate number of turns in the pickup coil and also the resistive load is determined to maximize the output power.

2. Modeling

As depicted in Fig. 1, the proposed device is a slim steel cantilever beam laminated with 2605SC Metglas as the magnetostrictive material and the whole beam is surrounded by a pickup coil which is responsible of harvesting the induced current i(t) as a result of the variation of the magnetic field which is generated due to the mechanical strain in 2605SC Metglas as a result of base excitation $w_b(t)$.

The induced current to the pickup coil is then harvested through the output electric circuit. Fig. 2 depicts a schematic of the output circuit:

Considering inextensionality condition in the midplane, the relation between longitudinal and transversal deflection along the midplane is given by [17]:

$$\frac{\partial}{\partial x}u(x,t) = \sqrt{1-\left(\frac{\partial}{\partial x}w(x,t)\right)^2} - 1 \qquad (1)$$

Where u and w, are longitudinal and transversal displacements respectively. The equation of the motion is derived by means of Newton's method as follows:

Integrating Eq. (1) once with respect to x, and then differentiating with respect to time twice yields:

$$\frac{\partial^2}{\partial t^2}u(x,t) = \int_0^x \left(\frac{\partial^2}{\partial t^2}\left(\sqrt{1-\left(\frac{\partial}{\partial x}w(x,t)\right)^2}\right)\right)dx \qquad (2)$$

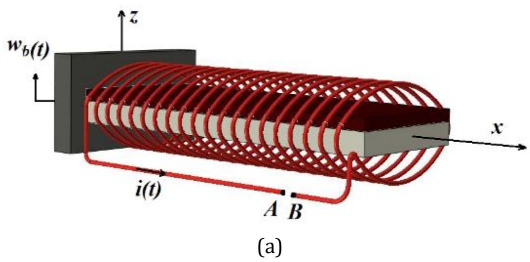

(a)

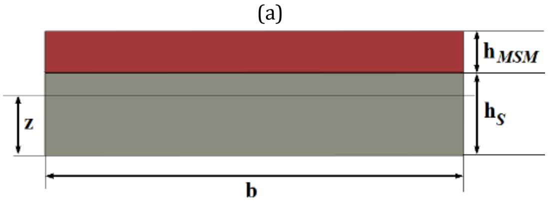

(b)

Fig. 1. a) 3-D model of magnetostrictive based energy harvesting device b) cross section

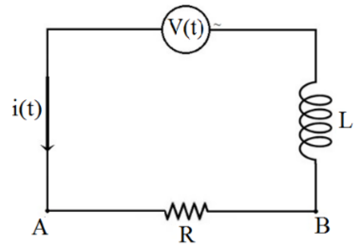

Fig. 2. Electric circuit corresponding to the model of magnetostrictive layer with dependent voltage source

Fig. 3 illustrates deformed and undeformed beam configurations and longitudinal and transverse displacements along with acting forces.

Considering Eq. (3), which is based on Fig. 3 and deduced by Nayfeh et al. [17]:

$$\cos\theta = 1 + \frac{\partial}{\partial x}u(x,t)$$
$$\sin\theta = \frac{\partial}{\partial x}w(x,t) \quad (3)$$
$$\theta = \theta(x,t)$$

and using Newton's second law according to Fig. 3 yields:

$$\frac{\partial}{\partial x}(N\cos\theta) - \frac{\partial}{\partial x}(V\sin\theta) = m\frac{\partial^2}{\partial t^2}u(x,t) \quad (4)$$

$$\frac{\partial}{\partial x}(N\sin\theta) + \frac{\partial}{\partial x}(V\cos\theta) + F_{ext} = m\frac{\partial^2}{\partial t^2}w(x,t) \quad (5)$$

$$\frac{\partial}{\partial x}M + V = J\frac{\partial^2}{\partial t^2}\theta(x,t) \quad (6)$$

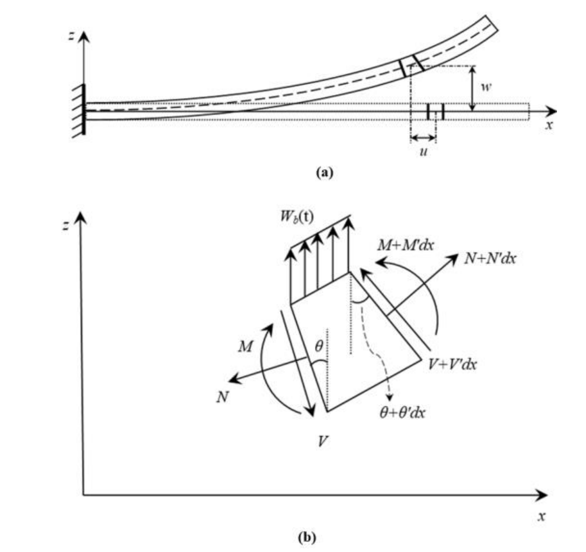

Fig. 3 a) longitudinal and transversal deflection b) Free body diagram of deformed segment of beam

Where V, N, m are shear force, axial force and mass of a unit length, respectively. M is the bending moment evaluated as:

$$M = b\left(\int_{-\bar{z}}^{h_S-\bar{z}} \sigma_{MSM} z dz + \int_{h_S-\bar{z}}^{h_S+h_{MSM}-\bar{z}} \sigma_S z dz\right) \quad (7)$$

$$m = b(h_S\rho_S + h_{MSM}\rho_{MSM}) \quad (8)$$

Where subscripts MSM and S stands for magnetostrictive and steel materials respectively. σ and ρ represent stress and mass density. $\bar{z}$ is the distance from neutral axis to the end of steel part of the beam. Stress is related to the strain for each material as:

$$\begin{Bmatrix}\sigma_{MSM}\\ B\end{Bmatrix} = \begin{bmatrix}E_{MSM}^H & -e\\ e^* & \mu^s\end{bmatrix}\begin{Bmatrix}\varepsilon\\ H\end{Bmatrix} \quad (9)$$

$$\sigma_S = E_S\varepsilon \quad (10)$$

Where E_S and E_{MSM}^H represents Young's modulus of elasticity of steel and magnetostrictive material in constant magnetic field respectively. $e^*$and e are two material constants and assumed to be equal for small strains [7]. μ^s is magnetic permeability under constant strain. B, H and ε, respectively stand for magnetic flux density, magnetic field and strain. Stress components are determined based on standards [18]. The Magnetic field is related to the electrical current according to Eq. (11) based on Faraday's law , and ε is given as Eq. (12).

$$H(t) = \frac{Ni(t)}{l} \quad (11)$$

$$\varepsilon = -z\frac{\partial}{\partial x}\theta \quad (12)$$

Where N is the number of turns of pickup coil. Substituting Eqs. 9 and 10 into Eq. 7, considering Eqs. 11 and 12, bending moment reduces to:

$$M = b\left(EI_{eq}\frac{\partial}{\partial x}\theta - \upsilon\big(\tilde{H}(x) - \tilde{H}(x-l)\big)\right) \quad (13)$$

Where $EI_{eq}$is the equivalent bending stiffness and $\tilde{H}$ is the Heaviside function which is implemented in the above equation in order to let the term survive through the differentiation.

$$EI_{eq} = \frac{b}{3}(E_S((h_S-\bar{z})^3 - \bar{z}^3) + E_{MSM}((h_{MSM}+h_S-\bar{z})^3 - (h_S-\bar{z})^3)) \quad (14)$$

and υ represents:

$$\upsilon = \frac{beN}{2l}((h_S+h_{MSM}-\bar{z})^2 - (h_S-\bar{z})^2) \quad (15)$$

Introducing Eq.13 into Eqs. 4-6, considering Eqs. 1-3 and expanding trigonometric relations in Taylor series, equation of motion reduces to:

$$-\frac{1}{2}\left[\frac{\partial}{\partial x}\left(\frac{\partial w(x,t)}{\partial x}\int_l^x m\left(\frac{\partial^2}{\partial t^2}\left(\int_0^x\left(\frac{\partial w(x,t)}{\partial x}\right)^2 dx\right)\right)\right)\right] \quad (16)$$

$$-EI_{eq}\frac{\partial}{\partial x}\left[\frac{\partial w(x,t)}{\partial x}\left(\frac{\partial^2 w(x,t)}{\partial x^2}\right)^2\right.$$

$$\left.+\frac{\partial^3 w(x,t)}{\partial x^3}+\frac{\partial^3 w(x,t)}{\partial x^3}\left(\frac{\partial w(x,t)}{\partial x}\right)^2\right]$$

$$+vi(t)\left[\left(\frac{d}{dx}\delta(x)-\frac{d}{dx}\delta(x-l)\right)\right.$$

$$\left(1+\frac{1}{2}\left(\frac{\partial w(x,t)}{\partial x}\right)^2\right)+$$

$$\left.(\delta(x)-\delta(x-l))\frac{\partial w(x,t)}{\partial x}\frac{\partial^2 w(x,t)}{\partial x^2}\right]$$

$$+J\left(\frac{\partial^4 w(x,t)}{\partial x^2\partial t^2}\right)+\mathrm{m}\frac{\partial^2 w_{\mathrm{b}}(\mathrm{t})}{\partial t^2}=-m\frac{\partial^2 w(x,t)}{\partial t^2}$$

Where the boundary conditions are as follows:

$$u(0,t)=0 \qquad w(0,t)=0 \qquad (17)$$

$$\frac{\partial}{\partial x}u(0,t)=0 \qquad \frac{\partial}{\partial x}w(0,t)=0 \qquad (18)$$

$$\frac{\partial^3}{\partial x^3}w(l,t)=0 \qquad \frac{\partial^2}{\partial x^2}w(l,t)=0 \qquad (19)$$

In order to derive reduced order model, we apply the Galerkin method together with normalized undamped beam's mode shapes as the shape functions. Following the procedure mentioned by S. Azizi et al. [19,20], deflection of the beam is expressed as:

$$w(x,t)=\sum_{i=1}^{n} q_i(t)\varphi_i(x) \qquad (20)$$

where $q_i(t)$ is the generalized coordinate. Substituting the approximate solution (Eq 20) into Eq 19, multiplying both sides in the shape function and integrating over the length, based on Galerkin method, the following reduced order model in terms of the generalized coordinates is obtained.

$$M_{nl}q(t)(q(t)\ddot{q}(t)+\dot{q}(t)^2)$$

$$-K_{nl}q(t)^3-K_l q(t)-Si(t)q(t)^2- \qquad (21)$$

$$Ti(t)+F_r(t)=M_l\ddot{q(t)}$$

Where upper dots denote derivative with respect to time and the coefficients of the equation are given as:

$$M_{nl}=-\int_0^l m\varphi(x)\left[\varphi''(x)\int_l^x\int_0^x\varphi(x)^2dx\,dx\right.$$

$$\left.+\varphi'(x)\int_0^x\varphi'(x)^2dx\right]dx \qquad (22)$$

$$K_{nl}=\int_0^l EI_{eq}\varphi(x)[4\varphi'(x)\varphi''(x)\varphi'''(x)$$

$$+\varphi'(x)^2\varphi''''(x)+\varphi''(x)^3]dx$$

$$K_l=\int_0^l EI_{eq}\varphi''''(x)dx$$

$$S=\int_0^l v\varphi(x)\left[\frac{1}{2}\varphi'(x)^2\left(\frac{d}{dx}\delta(x)\right.\right.$$

$$\left.-\frac{d}{dx}\delta(x-l)\right)$$

$$\left.+\varphi'(x)^2\varphi''(x)^2(\delta(x)-\delta(x-l))\right]dx$$

$$T=\int_0^l v\varphi(x)\left(\frac{d}{dx}\delta(x)-\frac{d}{dx}\delta(x-l)\right)dx$$

$$M_l=\int_0^l\varphi(x)(m\varphi(x)-J\varphi''(x))dx$$

$$F_r=\mathrm{m}\frac{\partial^2}{\partial t^2}w_{\mathrm{b}}(\mathrm{t})\int_0^l\varphi(x)dx$$

In Eq. 22 primes indicate derivatives with respect to x. The differential equation governing the electrical output current is derived based on Kirchhoff's law [21-22] as:

$$L\frac{di(t)}{dx}+Ri(t)+\sum_{r=1}^{n}\chi_r\dot{q}_r(t)=0 \qquad (23)$$

Where i and L are current and the equivalent inductance associated with the pickup coil respectively. L and χ_r are given as [22]:

$$L=\frac{\mu^s N^2 b h_{MSM}}{l} \qquad (24)$$

$$\chi_r=v\frac{d\varphi_r(x)}{dx}\bigg|_{x=l} \qquad (25)$$

3. Results and Discussions

Geometrical and mechanical properties of the case study are given in Table 1. To examine the energy conservation, as the first step initial energy is injected to the beam in terms of strain energy by means of a preliminary mechanical disturbance; once the disturbance is applied it is expected that the stored energy is picked up through the pickup coil as the magnetostrictive layer generates variable magnetic field around the beam and accordingly an electrical current is induced in the pickup coil.

Stored and harvested energy was in good agreement for different load resistance and number of turns in pickup coil. These results are given in Table 2.

Figure 4 depicts free vibration temporal response of the tip deflection of the beam, phase plane corresponding to the tip of the beam with N=1200 and R=1000 Ω; the initial tip disturbance of the beam is assumed to be 5cm.

Table 1. Mechanical and geometrical properties of the proposed magnetostrictive energy harvesting device

Characteristics	2605SC Metglas	Stainless Steel
Thickness h (mm)	0.2	0.8
Length l (mm)	200	200
Width b (mm)	10	10
Mass density (kg/m3)	7320	7850
Young modulus E (GPa)	110	220
Magnetomechanical coefficient (nm/A)	44000	___
permittivity	$0.03 \times \pi^2$	___

Table 2. Energy Conservation examination

Load Resistance	Number of turns in pickup coil	Harvested Energy (W)	Strain Energy (W)	Deference (%)
600	1200	0.0658	0.0627	0.3062
1000	1200	0.0657	0.0627	0.3060
1000	500	0.0657	0.0627	0.3029
300	200	0.0649	0.0627	0.2247
200	300	0.0658	0.0627	0.3054

Figure 5 illustrates the similar results as of Fig. 4 for R=1000 Ω and N=500, corresponding to same initial condition.

Figure 6 illustrates the temporal, phase plane responses, output current and power subjected to the same initial condition as of Figs. 3 and 4, and with R=600 Ω and N=1200

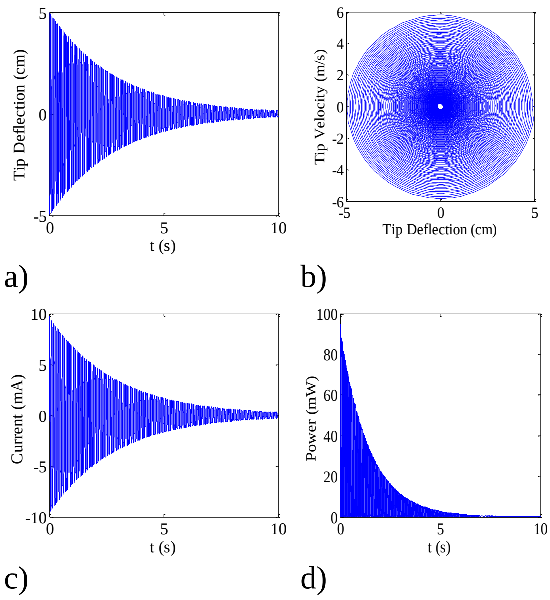

Fig. 4. Free oscillation response for *R=1000 Ω* and *N=1200* Generalized coordinates b) Phase Plane c) Output Current d) Output Power

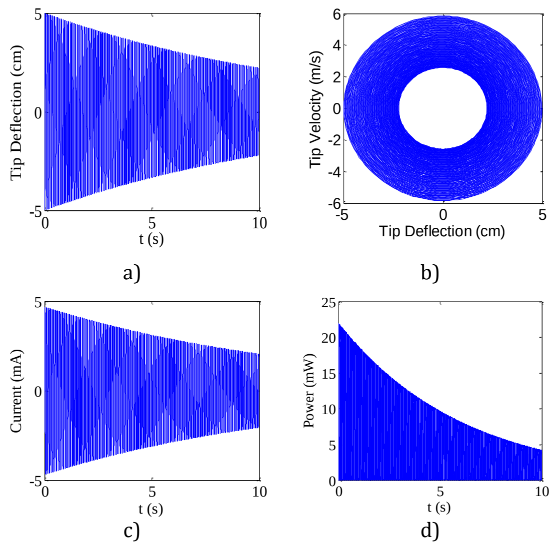

Fig. 5. Free oscillation response for *R=1000 Ω* and *N=500* Generalized coordinates b) Phase Plane c) Output Current d) Output Power

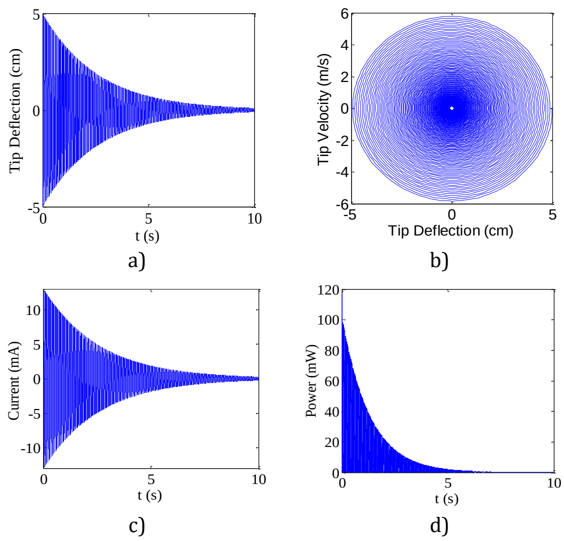

Fig. 6. Free oscillation response for *R=600 Ω* and *N=1200* a) Generalized coordinates b) Phase Plane c) Output Current d) Output Power

Comparing Figs. 3 - 5, it is observed that the attenuation rate of the response amplitude differs in each case; this means that due to the harvesting of the energy even though in the absence of any mechanical damping mechanisms, the overall mechanical energy of the beam attenuates and as a result the response amplitude descends; this fact encourages one to investigate the probable relation between resistive load, number of turns of pickup coil and the attenuation rate; to this end, in the absence of mechanical damping, attenuation rate is compared to that of mechanically-damped beam and the equivalent damping coefficient is determined for different resistance values and turns of pick up coil which is illustrated in Fig. 7.

Figure 8 depicts the equivalent damping coefficient versus number of pickup coils for different output resistances.

Figure 9 illustrates the equivalent damping coefficient versus resistive load for different number of pickup coils.

As depicted in Figs. 7-9, the equivalent damping ratio is dependent on the number of turns of the pickup coil as well as the output resistance. The maximum value of the damping ratio corresponding to the maximum harvested power, for different resistances and pickup coils are the same. Damping in terms of the number of turns in pickup coil regardless of resistive load exhibits a Lorentzian behavior as mentioned by Jafari et al. [16]. Seeking for an appropriate number of turns in the pickup coil and the corresponding value for the output resistance, to harvest the maximum possible power, we introduce the following relation:

$$R = 1.68N - 584 \quad (32)$$

This equation is deduced from the investigating the system with different values of resistance and number of pickup coils which is illustrated in Fig. 7. We fitted a curve on this diagram and found this relation to maximize the harvested energy. As the second part of this study, the system response is investigated once the device is subjected to harmonic base excitation and the frequency response is determined and compared to that of the linear model to show the effect of nonlinearity which dominates in case of large deformation problem.

Figure 10 depicts the frequency response of the tip deflection of the beam once the device is subjected to harmonic base excitation considering both linear and nonlinear formulation. It is worth mentioning that only the first mode effect is considered in the reduced order model. As it was reported by Nayfeh et al. [17], hardening effect was dominant in the first mode in the nonlinear model accounting for larger deformation problem.

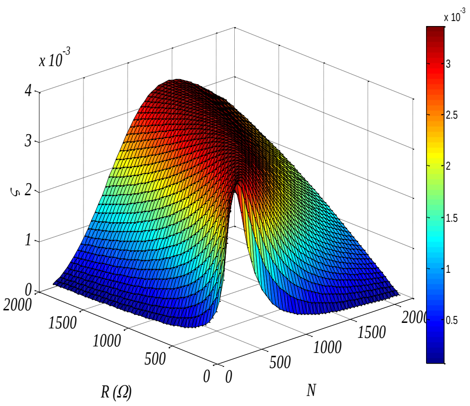

Fig. 7. Equivalent damping coefficient versus load resistance and number of pickup coils

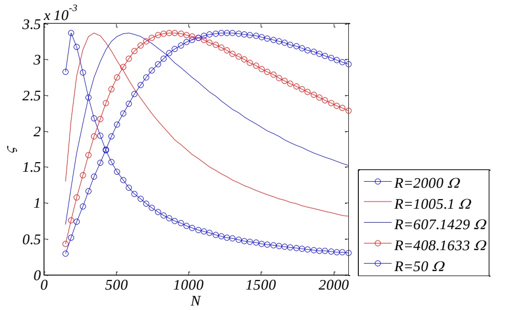

Fig. 8. Equivalent damping coefficient versus number of pickup coils

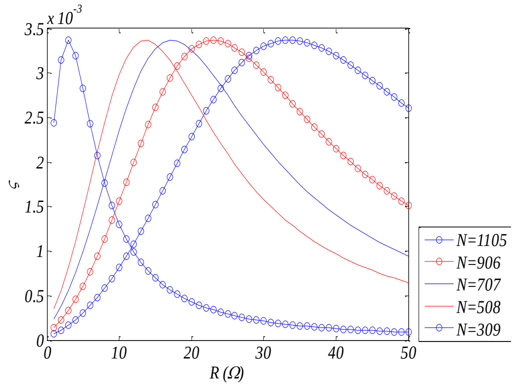

Fig. 9. Equivalent damping coefficient versus resistive load

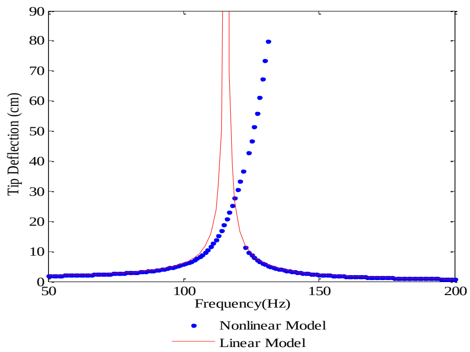

Fig. 10. Frequency response in the domain of first natural mode

The temporal response corresponding to forward and backward sweep in the vicinity of the first natural mode is depicted in Fig. 11 which shows hysteresis effect due to the nonlinearity of the response.

We have excited the device in the vicinity of the second natural frequency of the beam and accordingly accounted for the effect of the second mode in the reduced order model, as depicted in the Fig. 12 the beam exhibits softening response in the vicinity of the second natural mode indicating the domination of the softening effect of the nonlinear terms in the system response which is in agreement with what reported by Nayfeh et al. [17].

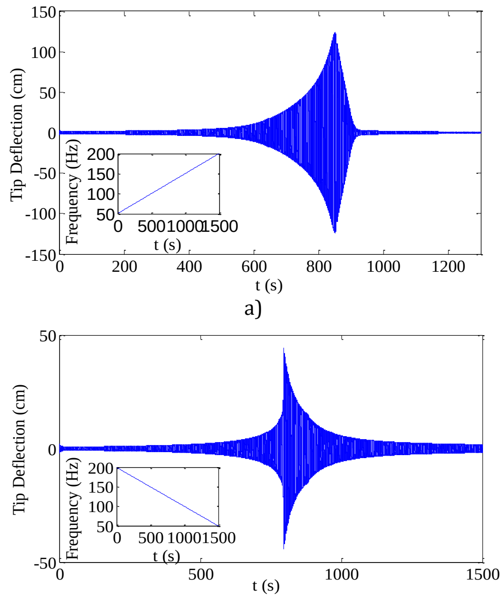

Fig. 11. a) Forward Sweep b) Backward Sweep

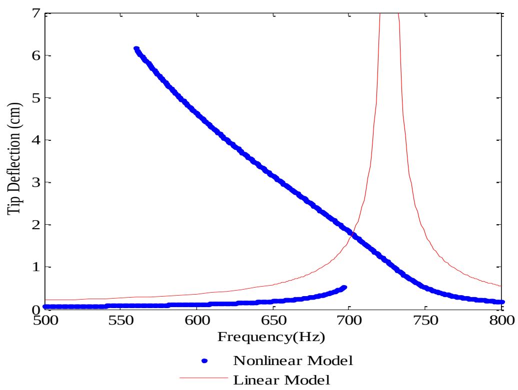

Fig. 12. Frequency response in the domain of second natural mode

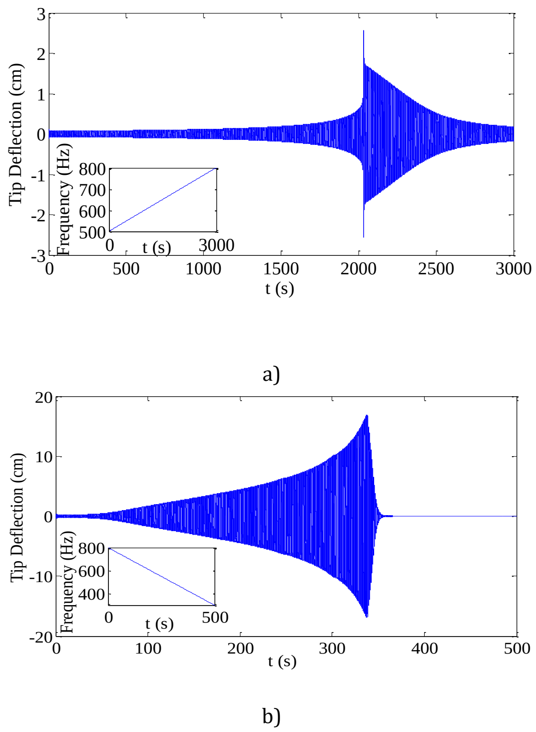

Fig. 13. a) Forward Sweep b) Backward Sweep

The time history of the forward and backward sweep in the domain of second mode and the corresponding frequency-time diagram is illustrated in Fig. 13 indicating the hysteresis due to the nonlinear behavior.

4. Conclusions

An energy harvesting device based on magnetostriction was proposed in this paper. The model was made up of a steel beam laminated with Metglas 2605sc as the magnetostrictive material throughout the entire length of the beam. The beam was surrounded with a pickup coil that was responsible for converting the energy of the magnetic field into electrical energy. The device was subjected to external base excitation which imposes mechanical strain to the Metglas material, and accordingly, a harmonic magnetic field is produced around the beam.

The energy of the magnetic field is converted to electrical energy throughout the output electrical circuit. The governing motion equations were derived based on Newton's motion law, considering the effects of nonlinear inertia and curvature, which dominates in the case of large-deformation problems. The motion equation was discretized to a reduced-order problem based on the Galerkin method, and the governing equations were numerically integrated over time to determine the temporal and frequency responses. The energy conservation was examined by imposing an initial disturbance to the tip of the beam; the harvested energy throughout the output circuit was compared to the injected initial strain energy. In the absence of mechanical damping, the beam's motion amplitude decayed over time which was attributed to the conversion of the mechanical energy into electrical energy utilizing an output circuit. The system response was compared to that of free vibrating single degree of freedom mass-spring-damper system, and the equivalent damping ratio was determined. The frequency response of the system was determined in the vicinity of first and second natural modes; the beam exhibited hardening and softening responses in the vicinity of the first and second natural modes respectively; this was attributed to the softening and hardening effects of the nonlinear inertia and curvature in the governing motion equations. The system response in the frequency domain, once the beam was exposed to a harmonic base excitation was determined. The effects of the number of turns in the pickup coil, output resistance, and the excitation frequency on the damping ratio, which was in direct relation with the output power, were investigated. The results of the present work can be used in design applications in future works.

References

[1] Joule, J. P., 1842. On a new class of magnetic forces. *Ann. Electr. Magn. Chem*, 8(1842), pp.219-224.

[2] Sadiku, M. N., 2014. Elements of electromagnetics. Oxford university press.

[3] Olabi, A. G. and Grunwald, A., 2008. Design and application of magnetostrictive materials. *Materials & Design*, 29(2), pp.469-483.

[4] Glynne-Jones, P., and White, N. M., 2001. Self-powered systems: a review of energy sources. *Sensor review*, 21(2), pp.91-98.

[5] Anshul, G. and Dwivedy, S. K., 2019. Nonlinear dynamics of parametrically excited piezoelectric energy harvester with 1: 3 internal resonance. *International Journal of Non-Linear Mechanics*, 111, pp. 82-94.

[6] Rojas, E. F., Faroughi, S., Abdelkefi, A. and Park, Y. H., 2019. Nonlinear size dependent modeling and performance analysis of flexoelectric energy harvesters. *Microsystem Technologies*, 25, pp.3899-3921.

[7] Leadenham, S.,and Erturk, A. 2020. Mechanically and electrically nonlinear non-ideal piezoelectric energy harvesting framework with experimental validations. *Nonlinear Dynamics*, 99, pp.625-641.

[8] Faroughi, S., Rojas, E. F. and Abdelkefi, A. 2019. Reduced-order modeling and usefulness of non-uniform beams for flexoelectric energy harvesting applications. *Acta Mechanica*, 230, pp.2339-2361.

[9] Sodano, H. A., Inman, D. J. and Park, G., 2004. A review of power harvesting from vibration using piezoelectric materials. Shock and Vibration Digest, 36(3), pp.197-206.

[10] Mohammadi, S. and Esfandiari, A., 2015. Magnetostrictive vibration energy harvesting using strain energy method. *Energy*, 81, pp.519-525.

[11] Wang, L. and Yuan, F. G., 2008. Vibration energy harvesting by magnetostrictive material. *Smart Materials and Structures*, 17(4), 045009.

[12] Staley, M. E. and Flatau, A. B., 2005. Characterization of energy harvesting potential of Terfenol-D and Galfenol. *Proceedings of the SPIE*, 5764, pp. 630-640.

[13] Adly, A., Davino, D., Giustiniani, A. and Visone, C., 2010. Experimental tests of a magnetostrictive energy harvesting device toward its modeling. *Journal of Applied Physics*, 107(9), 09A935.

[14] Davino, D., Krejčí, P., Pimenov, A., Rachinskii, D. and Visone, C., 2016. Analysis of an operator-differential model for magnetostrictive energy harvesting. *Communications in Nonlinear Science and Numerical Simulation*, 39, pp.504-519.

[15] Davino, D., Giustiniani, A. and Visone, C., 2012. Effects of hysteresis and eddy currents in magnetostrictive harvesting devices. *Physica B: Condensed Matter*, 407(9), pp.1433-1437.

[16] Talleb, H. and Ren, Z., 2014. Finite element modeling of magnetoelectric laminate composites in considering nonlinear and load effects for energy harvesting. *Journal of Alloys and Compounds*, 615, pp.65-74.

[17] Nierla, M., Löffler, M. and Rupitsch, S. J., 2015. Iterative finite element scheme for magnetoelectric energy harvesters. *Procedia Engineering*, 120, pp.496-500.

[18] Borowiec, M. and Syta, A., 2016. Modelling of Energy Harvesting System from Vertically Excited Magnetostrictive Beam. *Trans Tech Publications In Applied Mechanics and Materials*, 844, pp. 128-137.

[19] Jafari, H., Ghodsi, A., Azizi, S. and Ghazavi, M. R., 2017. Energy harvesting based on magnetostriction, for low frequency excitations. *Energy*, 124, pp.1-8.

[20] Nayfeh, A. H. and Pai P. F., 2004. Linear and Nonlinear Structural Mechanics. Wiley Series in Nonlinear Science. Hoboken, N.J., Wiley-Interscience.

[21] Cain, M. G. and Stewart, M., 2014. Standards for Piezoelectric and Ferroelectric Ceramics. in Characterisation of Ferroelectric Bulk Materials and Thin Films, ed: Springer, pp. 267-275.

[22] Azizi, S., Ghazavi, M. R., Rezazadeh, G., Ahmadian, I. and Cetinkaya, C., 2014. Tuning the primary resonances of a micro resonator, using piezoelectric actuation. *Nonlinear dynamics*, 76, pp.839-852.

[23] Chorsi, M. T., Azizi, S. and Bakhtiari-Nejad, F., 2015. Application of quadratic controller to control the pull-in instability of a micro-resonator. International *Journal of Mechanics and Materials in Design*, 11, pp.111-123.

[24] Desoer, C. A., 2009. Basic circuit theory. Tata McGraw-Hill Education.

[25] Cheng, D. K., 1989. Field and wave electromagnetics. Pearson Education India.